Lithium Batteries

DOI: 10.1002/anie.201300680

Lithium Polysulfidophosphates: A Family of Lithium-Conducting Sulfur-Rich Compounds for Lithium–Sulfur Batteries**

*Zhan Lin, Zengcai Liu, Wujun Fu, Nancy J. Dudney, and Chengdu Liang**

The conflict of the ever-increasing demand of energy consumption and the public concern over environmental issues demands a sustainable energy future that requires innovations on harvesting and delivering clean energies. Batteries have been brought into the spotlight as the pivotal technology for the electricity-based energy infrastructure that incorporates intermittent renewable energies. Although lithium ion (Li-ion) batteries have succeeded in powering personal electronics and small electric tools, they face the challenges of safety, cost, and energy density for the needs of independent electrified transportation and large-scale energy storage.[1] As compared to the current Li-ion batteries, Lithium–sulfur (Li-S) batteries are a promising candidate technology with advantages of abundant materials and inherently high energy. However, achieving longevity of cycling in Li-S batteries is formidable because of the electrical insulating nature of elemental sulfur and the poor ionic conductivity of sulfur and its discharge products. After nearly four decades of research, significant progress has been made to Li-S batteries: various carbon materials and conducting polymers impart electronic conductivity to the sulfur cathode,[2] and organic liquid electrolytes with good solubility to lithium polysulfides overcome the poor ionic conductivities of the sulfur cathode.[3] Using a liquid electrolyte that dissolves lithium polysulfides is a necessity in cycling conventional Li-S batteries: sulfur is actually cycling as a solution, also known as the catholyte.[4] The dissolved polysulfides move sulfur inside the electrochemical cells, which leads to parasitic side reactions that have been well-documented as the polysulfide shuttle (PS).[5] The short cycle-life and low energy efficiency of Li-S batteries is rooted in the PS phenomenon that is cause by the use of liquid electrolyte. Furthermore, stable long-term cycling of metallic lithium anode in some organic liquid electrolytes such as carbonate-based electrolytes, is a long-standing problem owing to the formation of an unstable solid electrolyte interphase and the dendritic growth of lithium deposition.[6]

Using solid electrolytes in Li-S batteries breaks the standard of conventional Li-S batteries. This game-changing shift from liquid to solid electrolytes eliminates the polysulfide shuttle and enables stable cycling of metallic lithium anodes. With the emergence of solid electrolytes with ionic conductivities comparable to that of liquid electrolytes,[7] all-solid-state Li-S batteries promise to be the next breakthrough for electric energy storage.[8] As in conventional Li-S batteries, the cycling of all-solid-state Li-S batteries has to overcome the poor electronic and ionic conductivities of the sulfur cathode. Seamless transport of ions and transfer of electrons are basic requirements for batteries. Although the electronic conductivity of the sulfur cathode can be improved by add carbon to the cathode, the ionic conductivity of sulfur cannot be significantly improved by the simple mixing of solid electrolytes with sulfur. There is a critical knowledge gap concerning the ionic conductivity of the sulfur cathode at the solid state. We report herein the first series of sulfur-rich compounds that have high ionic conductivities and excellent electrochemical reversibility during battery cycling.

Elemental sulfur (S_8) reacts with lithium thiophosphate (Li_3PS_4) in tetrahydrofuran (THF) following the equation in Scheme 1a. The reaction occurs at the negatively charged terminal sulfur atoms of PS_4^{3-}. Polysulfidophosphate anions

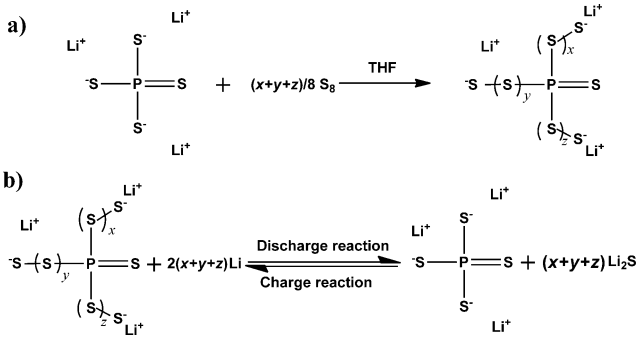

Scheme 1. Chemical reactions of lithium polysulfidophosphates (LPSPs). a) Reaction of sulfur with Li_3PS_4 yields Li_3PS_{4+n}, $n=(x+y+z)/3$, at room temperature in THF. Formation of the S–S bonds links S atoms to the core PS_4 unit. b) The electrochemical reaction mechanism for charge and discharge of Li_3PS_{4+n}. Reversible scission and formation of S–S bonds in LPSP.

[*] Dr. Z. Lin, Dr. N. J. Dudney
Materials Science and Technology Division
Oak Ridge National Laboratory
Oak Ridge, TN 37831-6124 (USA)
Dr. Z. Liu, Dr. W. Fu, Dr. C. Liang
Center for Nanophase Materials Sciences
Oak Ridge National Laboratory
Oak Ridge, TN 37831-6493 (USA)
E-mail: liangcn@ornl.gov

[**] This research was sponsored by U.S. Department of Energy (DOE)/ Energy Efficiency and Renewable Energy (EERE) through Vehicle Technologies Office. The investigation of the ionic conductivity of these new compounds was supported by the Division of Materials Science and Engineering, Office of Basic Energy Sciences, U.S. Department of Energy (DOE). The synthesis and characterization was conducted at the Center for Nanophase Materials Sciences, which is sponsored at Oak Ridge National Laboratory by the Division of Scientific User Facilities, U.S. DOE.

Supporting information for this article is available on the WWW under http://dx.doi.org/10.1002/anie.201300680.

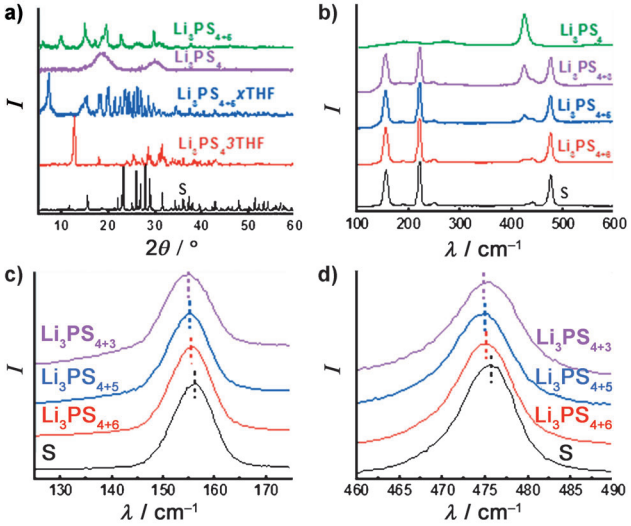

Figure 1. XRD patterns and Raman spectra to confirm the formation of lithium polysulfidophosphates. a) XRD patterns of S, Li_3PS_4 and Li_3PS_{4+n} ($n=5$) with/without THF; b) Raman spectra of S, Li_3PS_4, and Li_3PS_{4+n} ($n=3$, 5, and 6); c), d) Raman shift between the wavelengths of c) 125–175 cm^{-1} and d) 460–490 cm^{-1}.

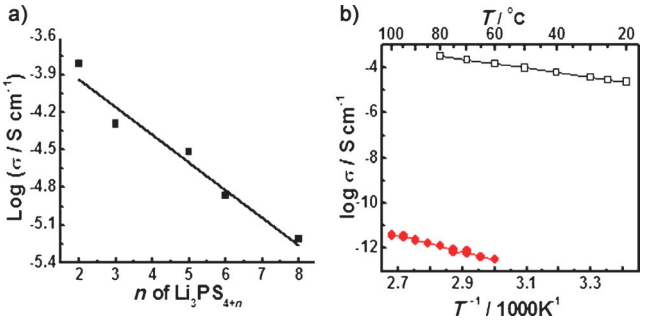

Figure 2. Conductivity of lithium polysulfidophosphates. a) Room-temperature ionic conductivity as a function of n (S–S bonds) in Li_3PS_{4+n} ($n=2$, 3, 5, 6, and 8) at 25 °C. b) Temperature dependency of ionic conductivity of Li_3PS_{4+5} (□, $E_a=0.37$ eV) and Li_2S (●, $E_a=0.74$ eV).

are formed through the formation of S–S single bonds. The reaction products are lithium polysulfidophosphates (LPSP), which have the general formula Li_3PS_{4+n} ($0<n<9$). The n in the formula represents the number of S–S bonds in the LPSP molecule. X-ray diffraction (XRD) and Raman spectra in Figure 1 verify the formation of this new family of sulfur-rich compounds. Comparing the XRD patterns of sulfur and Li_3PS_4·3 THF in Figure 1 a, a new crystalline structure of the sulfur compound Li_3PS_{4+n}·x THF ($n=5$) is apparent in the reaction. After the removal of THF at 80 °C under vacuum, the parent compound Li_3PS_4 becomes amorphous while the Li_3PS_{4+n} ($n=5$) is in crystalline form. Raman spectra (Figure 1 b) of Li_3PS_{4+n} ($n=3$, 5, and 6) show the symmetric stretching of the P–S bond at 418 cm^{-1} and the stretching vibrations of the P–S bond of 184 cm^{-1} regardless of number of sulfur atoms attached to the PS_4^{3-} anion.[9] With striking contrast to Li_3PS_4, the peaks centered at 155, 218/476, and 248/437 cm^{-1} appear for the LPSP compounds. These peaks are signatures of the E_2, A_1, and E_3 symmetry species of the S–S bond and confirm the formation of polysulfidophosphate anions.[10] With a decrease in sulfur atoms in LPSP compounds, the S–S bond peaks at 155 and 476 cm^{-1} shift to lower wavelengths (Figure 1 c,d). The downshifting of these peaks results from the vibrational effect of the P–S bond in core PS_4 unit and the increase in the sulfur chain length at the terminals.[11]

These LPSP compounds are lithium-ion conductors with room-temperature ionic conductivity in the range of 10^{-4} to 10^{-6} S cm^{-1} depending on the number of sulfur atoms. The correlation of ionic conductivity to the number of additional sulfur atoms incorporated into the parent compound Li_3PS_4 is shown in Figure 2 a. The log scale of the ionic conductivity ($\log\sigma$) of LPSP follows a linear relationship with the number of sulfur atoms (n) described in Equation (1):

$$\log\sigma = -3.486 - 0.219\,n \quad (1)$$

Temperature dependence of ionic conductivity was investigated for Li_3PS_{4+5} (Figure 2 b). This compound has a room-temperature ionic conductivity of 3.0×10^{-5} S cm^{-1} at 25 °C. The activation energy was derived from Arrhenius equation:

$$\sigma = A\exp(-E_a/kT) \quad (2)$$

Where σ is the ionic conductivity, T is the absolute temperature, k is the Boltzmann constant, A is the pre-exponential factor, and E_a is the activation energy. When $\log\sigma$ is plotted against $1/T$, a straight line is expected with a slope of $-E_a/k$ and an intercept of $\log A$. The calculated activation energy from Figure 2 b is 0.37 eV, which is comparable to that of the lithium super ionic conductor (LiSICON).[12] The ionic conductivity of Li_3PS_{4+5} is increased by a factor of 10 when the temperature is raised to 60 °C. As a comparison, we measured the ionic conductivity of Li_2S, the discharge product of elemental sulfur, at the same conditions. As shown in Figure 2 b, the ionic conductivity of LPSP is 8 orders of magnitude higher than that of Li_2S (ca. 10^{-13} S cm^{-1} at 25 °C).

Excellent cyclability was demonstrated using the compound Li_3PS_{4+5} as the cathode material at room temperature. The cathode shows an initial discharge capacity of 1272 mAh g^{-1} (based on the incorporated sulfur content) or 599 mAh g^{-1} (based on the compound; Figure 3 a) with 100 % of coulombic efficiency after a few initial cycles (Supporting Information, Figure S1; unless otherwise noted, the capacities hereafter are normalized to the sulfur content within the compound; for convenience, the normalized capacities based on the sulfur compound are also shown in figures). The cathode capacity stabilizes at 700 mA h g^{-1} after 300 cycles. Even better cycling performance was observed at 60 °C. The initial capacity was over 1400 mA h g^{-1}. A high capacity of 1200 mA h g^{-1} was maintained after 300 cycles. This observation confirms that the LPSP has an extremely stable cycling performance. The improved cycling performance is attributed to the increased ionic conductivity of both the solid electrolyte and the sulfur-rich cathode at 60 °C. Increased temperature may favor the electrochemical reactions as well. Polarization of the cell was large at room temperature and significantly reduced at 60 °C. Energy efficiency was

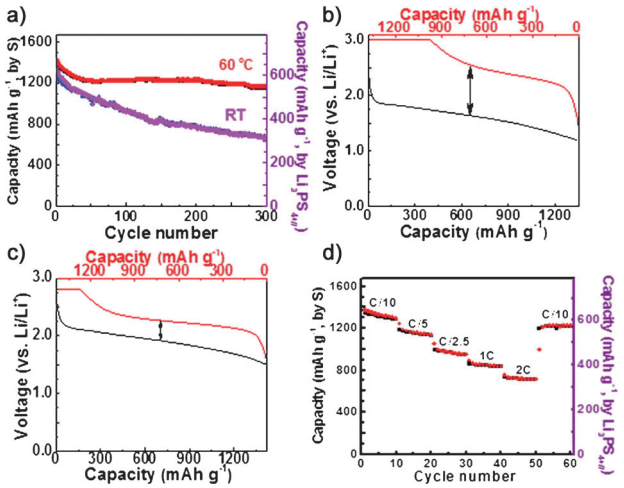

Figure 3. Electrochemical evaluation of Li_3PS_{4+5} as the cathode for all-solid-state Li-S batteries. a) The cycling performance at the rate of *C*/10 at room temperature and 60 °C (pink/red charge, black/blue discharge); b) representative voltage profile at room temperature (red charge, black discharge); c) representative voltage profile at 60 °C; and d) the rate performance at 60 °C from *C*/10 to 2C.

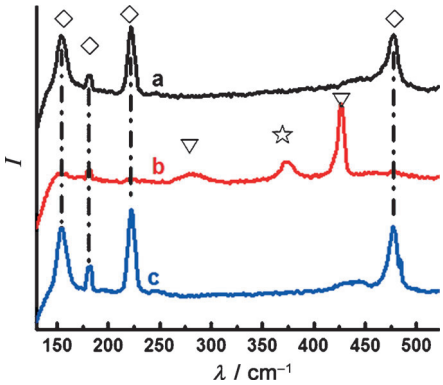

Figure 4. Raman spectra to unravel the electrochemical cycling mechanism. Raman spectra of the electrode materials consisting of carbon and Li_3PS_{4+n} ($n=5$) before cycling (a), at the end of first discharge cycle (b), and at the end of first charge cycle (c). ◇ peaks from the S–S bond in Li_3PS_{4+n}, ▽ peaks from the P–S bond in Li_3PS_4, ☆ the peak of Li_2S.

improved from 59.7 % at room temperature to 82.8 % at 60 °C (Figure 3 b,c). A good rate performance at 60 °C is shown in Figure 3 d. The cell has a capacity over 1200 mA h g^{-1} at *C*/10 and shows a reversible capacity of 735 mA h g^{-1} at 2*C* after 50 cycles at various rates. Further cycling at a low rate of *C*/10 brings it back to a reversible capacity of 1200 mA h g^{-1}. A control experiment using Li_3PS_4 and carbon material at 60 °C showed negligible capacity contribution from carbon (Supporting Information, Figure S2). In a conventional Li-S battery, the dissolution and migration of sulfur species cause the cathode structure to deteriorate which leads to a short cycle-life. Conversely, the integrity of the LPSP cathode structure was preserved after 300 deep cycles at 60 °C. SEM images and elemental maps of the pristine LPSP cathode and the LSPS cathode after 300 cycles are compared in the Supporting Information, Figure S3. No distinct difference was observed in these images.

The voltage profile of the LPSP cathode does not show two voltage plateaus that are normally observed in conventional Li-S batteries. The difference in voltage profiles of LPSP and conventional S indicates the electrochemical reaction of LPSP follows a different reaction pathway. The speculated reaction mechanism is depicted in Scheme 1 b; the reversible scission and formation of S–S bonds at the terminal S atoms accounts for the discharge/charge of LPSP. To unravel the charge/discharge mechanism of these sulfur-rich compounds, Raman spectra (Figure 4) were taken on the pristine material and at the end of each of the charge and discharge cycles. The peaks centred at 155, 218/476, and 180 cm^{-1} of the pristine Li_3PS_{4+5} are attributed to the S–S bond. After the first discharge cycle, the characteristic peaks of the S–S bond at 155, 218/476, and 180 cm^{-1} had vanished. New strong peaks at 375 and 418 cm^{-1} and a weak peak at 283 cm^{-1} appeared as evidence of the formation of Li_2S and Li_3PS_4. The discharge process breaks the S–S bond in Li_3PS_{4+5} and yields Li_2S and Li_3PS_4. When the cathode was charged again, S–S bond features reappeared with the disappearance of Li_2S and Li_3PS_4 at the end of the charge cycle. The Raman spectra of the pristine material and the charged cathode are very much the same. These Raman spectra confirmed that the electrochemical insertion and removal of lithium ion in the cathode is a reversible reaction of Li_3PS_{4+5} to a mixture of Li_2S and Li_3PS_4. The electrochemical scission and formation of S–S bonds are consistent with the reports of cycling organosulfur compounds with the thiol (–SH)/disulfide (S–S) redox couple.[13]

In summary, elemental sulfur reacts with Li_3PS_4. The reaction adds sulfur atoms to the charged terminal S atoms of PS_4^{3-} anion by forming S–S bonds. The addition of sulfur to PS_4^{3-} yields a new family of sulfur-rich compounds. These compounds have a lithium-ion conductivity in the range of 10^{-5} to 10^{-6} S cm^{-1} that is comparable to that of conventional Li-ion cathode materials, such as lithium metal oxides and phosphates. Reversible electrochemical reactions occur through the breaking and forming S–S bonds in LPSP compounds when they are applied as the cathode materials for all-solid-state Li-S batteries. These materials are excellent cathode materials for such Li-S batteries with an impressive cyclability. The ionic conductivity of the sulfur cathode is of paramount importance in the cycling of these Li-S batteries. However, this topic has been rarely studied for conventional Li-S batteries. This research bridges the knowledge gap between convention Li-S batteries and the new trend of all-solid-state Li-S batteries.

Experimental Section

Li_3PS_4 was prepared by a procedure described previously.[14] The sulfur compounds Li_3PS_{4+n} ($n=2,3,5,6$, and 8) were synthesized through solution reactions of Li_3PS_4 and elemental sulfur in tetrahydrofuran (THF) under magnetic stirring without exposure to air or moisture. After the solids were fully dissolved, the solution was dried under vacuum for 2 h at 80 °C. The recovered solids were lithium polysulfidophosphates. The cathode slurry was prepared by dispersing Li_3PS_{4+5} (60 wt %), WVA-1500 carbon (MeadWestvaco

Corporation, 30 wt%), and PVC binder (10 wt%) in THF. No side reaction occurred to the binder during the preparation of electrode because of the rapid evaporation of solvent.[15] A solid electrolyte pellet of Li_3PS_4 with a lithium metal anode was prepared by cold-pressing nanoporous β-Li_3PS_4 (120 mg) on top of a thin lithium foil (50 μm thick) under 240 MPa pressure in a 13 mm die. The slurry was then coated on the other side of the pellet and dried under vacuum at 80 °C. The loading of the cathode materials is 0.25–0.60 mg cm^{-2}, which is equivalent to 0.15–0.36 mAh cm^{-2}. The final thickness of the pellets was 0.5 mm.

The ionic conductivity of LPSP compounds was conducted in the frequency range of 10 MHz to 1 Hz with an amplitude of 10 mV by using a frequency response analyzer (Solartron 1260). Swagelok cells were used to evaluate the cycling performance. Carbon-coated aluminum foil (samples kindly provided by Exopack Advanced Coating) was used as the current collector. Charge and discharge cycles were carried out using a Maccor 4000 series battery tester at a current density of 0.015 mA cm^{-2} (*C*/10) between the cut-off potentials of 1.5–2.8 V vs. Li/Li$^+$. The current densities of 0.03 (*C*/5), 0.075 (*C*/2.5), 0.15 (*C*), and 0.2 (2*C*) mA cm^{-2} were applied to measure the rate performance of the LPSP cathode. The calculation of specific charge/discharge capacities was based on the mass of sulfur and the compound, respectively.

The morphologies of the cathode before and after cycling were examined using a field emission scanning electron microscope (FE-SEM; Zeiss Merlin) at 15 kV. The elemental maps of carbon, sulfur, and phosphorus were taken using the energy-dispersive spectroscope of the FE-SEM. X-ray diffraction (XRD) analysis was performed using a PANalytical X′pert PRO 2-circle X-ray diffractometer with a $Cu_{K\alpha}$ source ($\lambda \approx 1.5418$ Å). Raman spectroscopy was recorded from 600 to 100 cm^{-1} on a Renishaw Confocal MicroRaman spectrometer at room temperature. A green laser with wavelength of 532 nm was used for Raman excitation.

Received: January 25, 2013
Revised: March 6, 2013
Published online: June 4, 2013

Keywords: batteries · ionic conductivity · lithium · sulfidophosphates · sulfur

[1] a) M. Armand, J. M. Tarascon, *Nature* **2008**, *451*, 652–657; b) L. W. Ji, Z. Lin, M. Alcoutlabi, X. W. Zhang, *Energy Environ. Sci.* **2011**, *4*, 2682–2699.

[2] a) X. L. Ji, K. T. Lee, L. F. Nazar, *Nat. Mater.* **2009**, *8*, 500–506; b) G. Y. Zheng, Y. Yang, J. J. Cha, S. S. Hong, Y. Cui, *Nano Lett.* **2011**, *11*, 4462–4467; c) J. C. Guo, Y. H. Xu, C. S. Wang, *Nano Lett.* **2011**, *11*, 4288–4294; d) J. Wang, S. Y. Chew, Z. W. Zhao, S. Ashraf, D. Wexler, J. Chen, S. H. Ng, S. L. Chou, H. K. Liu, *Carbon* **2008**, *46*, 229–235; e) J. L. Wang, J. Yang, C. R. Wan, K. Du, J. Y. Xie, N. X. Xu, *Adv. Funct. Mater.* **2003**, *13*, 487–492; f) L. F. Xiao, Y. L. Cao, J. Xiao, B. Schwenzer, M. H. Engelhard, L. V. Saraf, Z. M. Nie, G. J. Exarhos, J. Liu, *Adv. Mater.* **2012**, *24*, 1176–1181; g) Y. Yang, G. H. Yu, J. J. Cha, H. Wu, M. Vosgueritchian, Y. Yao, Z. A. Bao, Y. Cui, *ACS Nano* **2011**, *5*, 9187–9193.

[3] a) J. Shim, K. A. Striebel, E. J. Cairns, *J. Electrochem. Soc.* **2002**, *149*, A1321–A1325; b) J. Gao, M. A. Lowe, Y. Kiya, H. D. Abruna, *J. Phys. Chem. C* **2011**, *115*, 25132–25137; c) Y. Jung, S. Kim, B. S. Kim, D. H. Han, S. M. Park, J. Kwak, *Int. J. Electrochem. Sci.* **2008**, *3*, 566–577; d) J. H. Shin, E. J. Cairns, *J. Power Sources* **2008**, *177*, 537–545.

[4] a) S. S. Zhang, J. A. Read, *J. Power Sources* **2012**, *200*, 77–82; b) S. S. Zhang, D. T. Tran, *J. Power Sources* **2012**, *211*, 169–172; c) Z. Lin, Z. Liu, W. Fu, N. J. Dudney, C. Liang, *Adv. Funct. Mater.* **2013**, *23*, 1064–1069.

[5] a) Y. V. Mikhaylik, J. R. Akridge, *J. Electrochem. Soc.* **2004**, *151*, A1969–A1976; b) S. S. Zhang, *Electrochim. Acta* **2012**, *70*, 344–348.

[6] D. Fauteux, R. Koksbang, *J. Appl. Electrochem.* **1993**, *23*, 1–10.

[7] N. Kamaya, K. Homma, Y. Yamakawa, M. Hirayama, R. Kanno, M. Yonemura, T. Kamiyama, Y. Kato, S. Hama, K. Kawamoto, A. Mitsui, *Nat. Mater.* **2011**, *10*, 682–686.

[8] a) T. Kobayashi, Y. Imade, D. Shishihara, K. Homma, M. Nagao, R. Watanabe, T. Yokoi, A. Yamada, R. Kanno, T. Tatsumi, *J. Power Sources* **2008**, *182*, 621–625; b) F. Mizuno, S. Hama, A. Hayashi, K. Tadanaga, T. Minami, M. Tatsumisago, *Chem. Lett.* **2002**, 1244–1245; c) J. Hassoun, B. Scrosati, *Adv. Mater.* **2010**, *22*, 5198–5201; d) Z. Lin, Z. Liu, N. J. Dudney, C. Liang, *ACS Nano* **2013**, *7*, 2829–2833.

[9] a) F. Mizuno, A. Hayashi, K. Tadanaga, M. Tatsumisago, *Adv. Mater.* **2005**, *17*, 918–921; b) A. Müller, N. Mohan, P. Cristoph, I. Tossidis, M. Drager, *Spectrochim. Acta Part A* **1973**, *29*, 1345–1356.

[10] a) D. W. Scott, F. H. Kruse, J. P. Mccullough, *J. Mol. Spectrosc.* **1964**, *13*, 313–320; b) A. T. Ward, *J. Phys. Chem.* **1968**, *72*, 4133–4139.

[11] R. Steudel, *Z. Naturforsch. B* **1975**, *30*, 281–282.

[12] G. Y. Adachi, N. Imanaka, H. Aono, *Adv. Mater.* **1996**, *8*, 127–135.

[13] a) Y. Nuli, Z. P. Guo, H. K. Liu, J. Yang, *Electrochem. Commun.* **2007**, *9*, 1913–1917; b) Y. J. Li, H. Zhan, L. B. Kong, C. M. Zhan, Y. H. Zhou, *Electrochem. Commun.* **2007**, *9*, 1217–1221.

[14] Z. Liu, W. Fu, E. A. Payzant, X. Yu, Z. Wu, N. J. Dudney, J. Kiggans, K. Hong, A. J. Rondinone, C. Liang, *J. Am. Chem. Soc.* **2013**, *135*, 975–978.

[15] G. X. Xu, L. Qi, B. T. Yu, L. Wen, *Chin. J. Polym. Sci.* **2006**, *24–3*, 307–313.

